Watt-level, green-pumped optical parametric oscillator based on periodically poled potassium titanyl phosphate with high extraction efficiency

Hang-Hang Yu(俞航航), Zhi-Tao Zhang(张志韬), and Hong-Wen Xuan(玄洪文)†

GBA Branch of Aerospace Information Research Institute, Chinese Academy of Sciences, Guangzhou 510700, *China*

(Received 3 July 2022; revised manuscript received 21 July 2022; accepted manuscript online 22 July 2022)

We report a compact, efficient optical parametric oscillator (OPO) based on a periodically poled potassium titanyl phosphate (PPKTP) crystal pumped by a 532 nm laser, which generated 1.51 W of average power at the signal wavelength of 709 nm with the pulse duration of ∼ 1.0 ns. The extraction efficiency was up to 59%. To the best of our knowledge, this is the first report on Watt-level green-pumped PPKTP-based singly resonant oscillator OPO (SRO-OPO). The precise build-up time of OPO was determined to be 1.6 ns benefitting from the characteristic of twin-peak pulse profile of pump beam. The spectrum width of the idler was also measured to be 4.2 nm with the central wavelength of 2134 nm at 0.2 nm spectral resolution of optical spectrum analyzer. In addition, the beam quality of $M^2 < 1.9$ of generated signal exhibits a good consistency with $M^2 < 1.5$ for the pump source.

Keywords: SRO-OPO, PPKTP, build-up time

PACS: 42.55.–f, 42.60.Jf, 42.65.–k **DOI:** 10.1088/1674-1056/ac8346

1. Introduction

In the past decades, visible laser has glorious applications in light communications, nonlinear spectroscopy and trace gas sensing.[1–3] Compact green-pumped optical parametric oscillators (OPOs) are proven way to generate short-pulse visible laser, which could also be as one of pumping sources for solid-state 193 nm laser generation. A green-pumped optical parametric oscillator (OPO) has the advantage of producing visible laser radiation directly as well as the tunability, owing to the current commercially available high-performance quasi-phase-matched (QPM) nonlinear materials such as periodically poled MgO-doped $LiNbO_3$ (MgO:PPLN), $LiTaO_3$ (PPLT), and $KTiOPO_4$ (PPKTP).[4–9] It provides broader solutions for realization of solid-state 193 nm laser or other deep ultraviolet lasers. Photorefractive effect and green-induced infrared absorption in PPLN and PPLT are inevitable, which hinder the OPO output power boosting, although the MgO-doped crystals have obtained extensive research due to their mature growth and poling technology.[10–12] Recently, PPKTP shows itself as a promising candidate for high power OPOs in visible and near-infrared range, not only for its high damage threshold but also for its high effective nonlinearity.[13,14] Notably, PPKTP has a higher photorefractive damage threshold and negligible green-induced infrared absorption compared to PPLN and PPLT. Table 1 summarizes the state-of-art OPOs based on PPKTP pumped by both CW- and pulsed-green laser. A CW green-pumped singly resonant oscillator OPO (SRO-OPO) based on PPKTP generated the signal at 946.4 nm with 28 mW under the pump power of 1.2 W, and the quantum efficiency was 13%.[15] For the dual-wavelength output by the green-pumped doubly resonant oscillator (DRO) OPOs based on PPKTP, the output power of the signal was from tens of mW to hundreds of mW.[16,17] Until now, the highest output signal power in the visible and near-infrared (below 1 μm) region is ∼ 580 mW at 765 nm.[18] In a word, the thermal effect inside PPKTP limits the OPO performances at high pumping power. High-power visible laser with good beam quality is the cornerstone to generate the 193 nm by single-step operation of sum frequency. However, there have been no reports on the Watt-level visible signal laser generated by green-pumped PPKTP-based OPOs seen from Table 1. The realization of Watt-level visible signal laser by PPKTP-based OPOs is still of challenge.

In this contribution, we demonstrate a Watt-level, nanosecond SRO-OPO employed a short cavity with a high conversion efficiency. A uniform grating-period PPKTP was applied to generate a signal light at 709 nm and an idler light at 2132 nm pumped by a 532 nm laser. The signal wavelength at 709 nm will be applied to the 193 nm generation by frequency mixing with the ultraviolet laser at 266 nm in further research, which is the second-harmonic wavelengths of the pump. Hence, the signal wavelength of 709 nm is fixed by keeping constant temperature and therefore the wavelength-tuning characteristic of crystal is needless. The average output power of the signal was 1.51 W with the repetition rate of 100 kHz and the pulse duration of ∼ 1 ns. To the best of our knowledge, this is the first report on Watt-level, nanosecond PPKTP-based SRO-OPO with a high pump extraction efficiency up to 59%. This system also has the potential for power scaling up to a higher level.

†Corresponding author. E-mail: xuanhw@aircas.ac.cn

© 2022 Chinese Physical Society and IOP Publishing Ltd

Table 1. The state-of-art OPOs based on PPKTP pumped by CW- and pulsed-green laser.

Pump wavelength (nm)	Pump mode	Signal (nm)	Idler (nm)	Signal power (mW)	Idler power (mW)
532[a]	CW	865–1032	1100–1384	28 (946.4 nm)	72 (1215 nm)
532[b]	CW	656–1035	1096–2830	60	800
532[c]	pulsed	726–955	1201–1998	580 (765 nm)	300 (1338 nm)
532[d]	CW	741–922	1258–1884	450@5 s (901 nm)	1200@5 s (1299 nm)

[a]Ref. [15], [b]Ref. [17], [c]Ref. [18], [d]Ref. [19].

2. Experimental setup

The experimental setup is schematically shown in Fig. 1. The pump is a commercially available diode-pumped-solid-state laser (DPSSL) operating at the central wavelength of 532 nm with about 3 ns pulse duration and 100 kHz repetition rate. The pumping source provides up to average power of 40 W with linearly polarization and in the approximate TEM_{00} spatial mode with $M^2 < 1.5$. The PPKTP crystal (Raicol Crystals Inc.) is 1 mm × 2 mm × 30 mm in dimensions with a domain inversion period of 11.05 μm. The crystal is mounted on a 40 mm-long copper oven with temperature tuning available from 20 °C to 60 °C by thermos-electric cooler (TEC) with the precision of 0.1 °C. Anti-reflective (AR) coating for 532 nm is applied to two end sides of the crystal. The OPO cavity has a length of ∼ 5.5 cm, and it is made up of a plane-convex dichromic mirror (DM) and a plane output coupler (OC). The dichromic mirror, with a radius of curvature of 2 m, is AR coated for 532 nm ($R < 0.5\%$). The OC is high reflective (HR) coating for 532 nm ($T < 0.2\%$) and partial reflective (PR) coating for the signal ($T = 35\%$). Both DM and OC mirrors are AR coated for idler (2143 nm) to form an SRO-OPO operation.

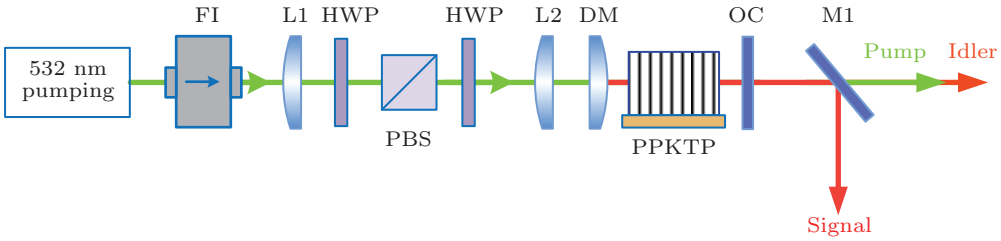


Fig. 1. Experimental setup of the green-pumped PPKTP OPO. FI, Faraday isolator; PBS: polarizing beam splitter; HWP: half-wave plate; DM: dichromic mirror; L: lens; M: mirror; OC: output coupler.

3. Results

Gauging the precise build-up time of OPO will play a significant role in SFG process of 193 nm generation in terms of the temporal overlap as well as the phase control. Due to the temporal gain narrowing effect, the pulse duration of the signal was shorter than that of the pump, making it an issue to have an exact measurement of OPO build-up time by our current photodiode (PD, Hamamatsu S5973-01). Benefitting from the stabilized twin-peak pulse profile of the pump, the estimation of the build-up time was feasible by our PD and oscilloscope. The pulse profiles of the pump and signal were measured by the fast response PD with the bandwidth more than 1 GHz and an oscilloscope (MSO44, Tektronix) to investigate the build-up time of OPO process, as shown in Fig. 2. The position of PD was fixed during measurement for depleted pump and signal pulse profile. Two dichromic mirrors with different coating (HR for 532 nm & HT for 709 nm, and HT for 532 nm & HR for 709 nm) were individually set before PD according to the necessity of measurement. For acquiring the high contrast data, the comparable amplitude responses of PD for the extraction pump and signal were required, which were achieved by using dichromic mirrors and polarization misalignment between pump and PPKTP crystal.

The pulse duration of the pump with twin-peak pulse profile before the OPO process was firstly measured to be 2.3 ns, as shown in Fig. 2(a). During the OPO process, the pulse profile was measured as depicted in Fig. 2(b) with a FWHM duration of right peak of 1.1 ns. Obviously, the pulse shape in Fig. 2(b) appears to have a similar twin-peak profile with the pulse shape of initial pump in Fig. 2(a) besides a larger right peak. After inserting a dichromic mirror (HT for 532 nm & HR for 709 nm) between PD and OPO cavity during the OPO process, the residual pulse profile shows a similar ratio twin-peak profile with initial pulse profile of pump shown in Fig. 2(a). Therefore, the pulse profile in Fig. 2(b) is verified to be the combination of the undepleted pump and the signal.

Pulse profiles in Figs. 2(a) and 2(b) are compared as shown in Fig. 2(c). The curves of A and B are the replica of Figs. 2(a) and 2(b), respectively. Curve C is the difference between B and A only by mathematical substraction. To further confirm that the pulse profile in Fig. 2(b) is the combination of the undepleted pump and the signal, the pulse duration of the signal shown in the left inset of Fig. 2(d) was measured to be of ∼ 1 ns after filtering out the undepleted pump by use of another dichromic mirror (HR for 532 nm & HT for 709 nm). The pulse profile of the measured signal is normalized and

demonstrated to be curve E in Fig. 2(d), and curve D is the normalization pulse profile of curve C. It is obvious that curves E and D fit with each other perfectly, which implies that the pulse shape in Fig. 2(b) is not only the undeleted pump but also with the signal. It is surprising that the pulse profile of signal is singlet instead of twin-peak pulse profile as pump. There is no reasonable explanation for this phenomenon. We notice that the slight humps exist on the right part in both curves D and E in Fig. 2(d), which may result from the right peak of pump pulse profile.

The right inset of Fig. 2(d) shows the residuals between D and E, which was supposed to be zero theoretically. It is mainly caused by the central peak mismatch and the intensity noise actually. To acquire the precise build-up time of OPO, we suppose that the singlet profile of signal arises from the left peak of pump pulse. Therefore, the build-up time of OPO could be obtained by the variation of curve E in delay time when the peak of the curve D coincides with the curve E in Fig. 2(d). The build-up time of OPO is certified with ~ 1.6 ns by the time variation of curve E.

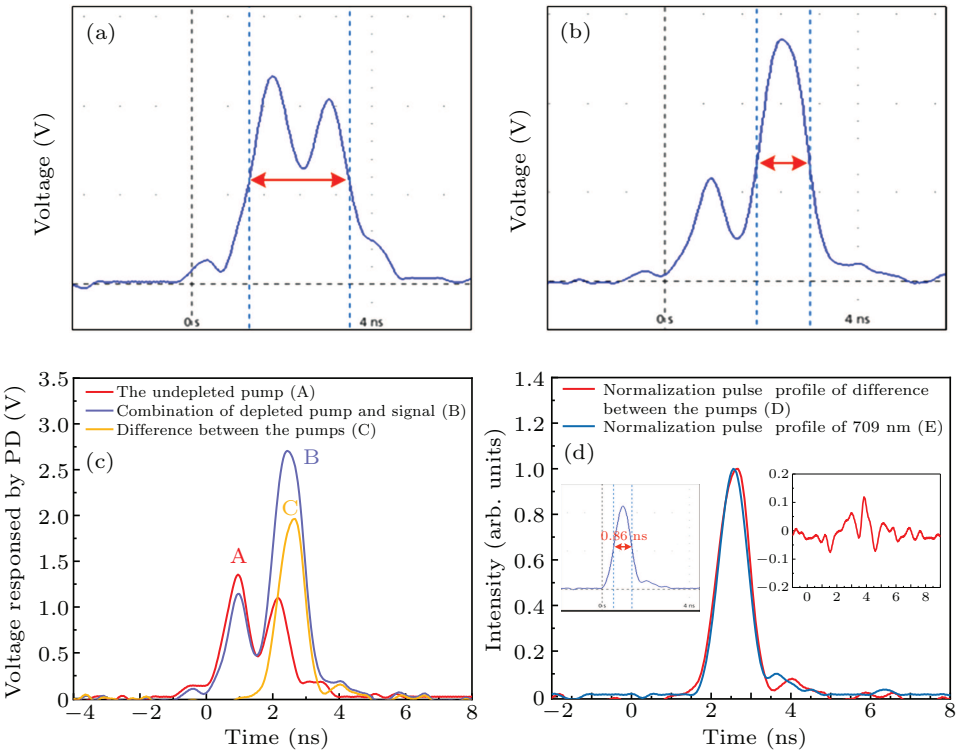


Fig. 2. Measured pulse profile of the pump and the signal. (a) The initial pulse profile of pump before the OPO process. (b) The combined pulse profile of signal and depleted pump during the OPO process. (c) The plots of detailed measurement data. (d) The comparison between the difference in (c) with individually measured signal pulse.

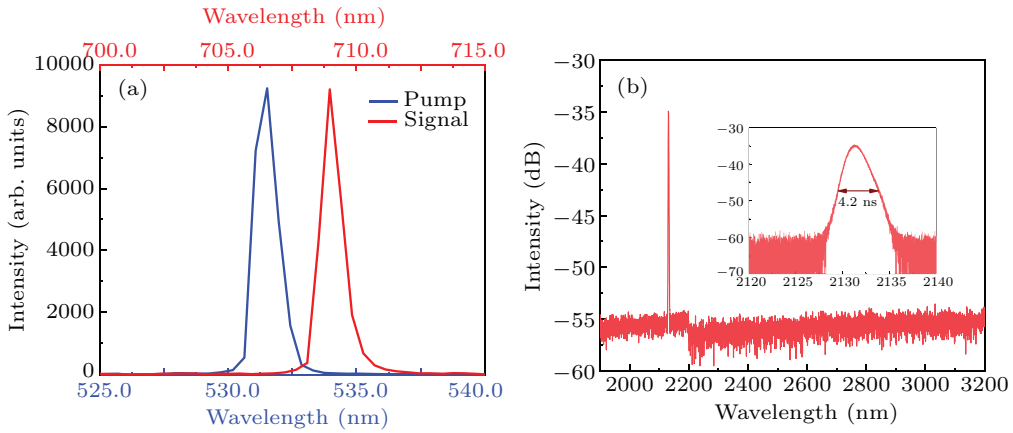


Fig. 3. The spectra of (a) pump and signal, and (c) idler.

The spectra of the pump and signal were measured using a spectrometer with the spectral resolution of 0.66 nm (HR4Pro, Ocean Optics). At the same time, the idler was checked by an optical spectrum analyzer (OSA, AQ6376, YOKOGAWA), as shown in Fig. 3. The central wavelengths for the pump and signal were 531.5 nm and 709 nm when the temperature of the

crystal was set to 60 °C. The spectrum width of the signal was ∼ 1 nm, which was narrower than that of pump with 1.2 nm. The inset in Fig. 3(b) is the enlarged view of idler showing SNR more than 20 dB, and the central wavelength of idler was 2132 nm with a spectrum width of 4.2 nm by using 0.2 nm resolution of OSA. The spectrum width of idler is obviously higher than that of the signal and pump, which may result from the associated effects of the non-monochromaticity of pump and QPM tolerability around central pump wavelength of PPKTP. It could contribute to multi-OPO processes within the spectrum width of pump.

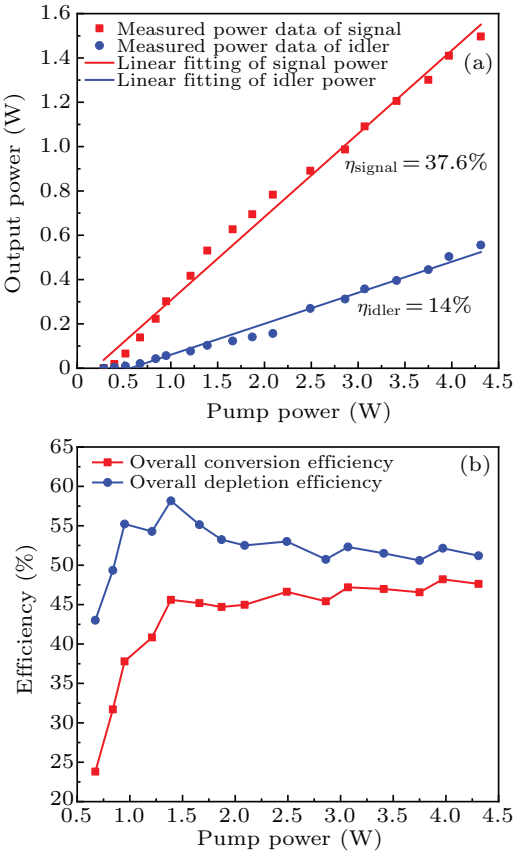


Fig. 4. Power scaling and efficiency of the OPO. (a) The output power and slope efficiency of signal and idler versus pump power. (b) The overall conversion and extraction efficiency versus pump power.

The signal and idler output powers were measured with results in Fig. 4. The temperature of PPKTP maintains at 60 °C. The maximum pump power was limited to 4.5 W to avoid excessive heat loading and the significant thermal lensing effect at high pump. With a single-side pump scheme, the OPO threshold is as low as ∼ 300 mW. The data-fitting slope efficiency of signal and idler are 37.6% and 14%, respectively, as illustrated in Fig. 4(a). At the pump power of 4.3 W, the signal and idler achieved the maximum output power of 1.51 W and 0.57 W, respectively. As shown in Fig. 4(b), the overall conversion and extraction efficiencies are $> 45\%$ and $> 52\%$, respectively, when the pump power is above 1.5 W. The output power and the extraction efficiency initially experiences a rapid increase, which leads to the maximum extraction efficiency up to 59 %. It is worth emphasizing that the measurement of idler power was only carried out after the OC without including the idler power on the pump-incidence side. Thus, it implies a higher idler power inside the SRO-OPO cavity. The overall efficiency continuously decreases because of the severe mode mismatch caused by the thermal lensing effect with pump power increasing. The slow downward trend of extraction efficiency benefits from the short cavity, which could eliminate the mode mismatch partially. Therefore, a higher conversion efficiency could be obtained when the mode mismatch is improved by selecting appropriate pump parameters in the further research.

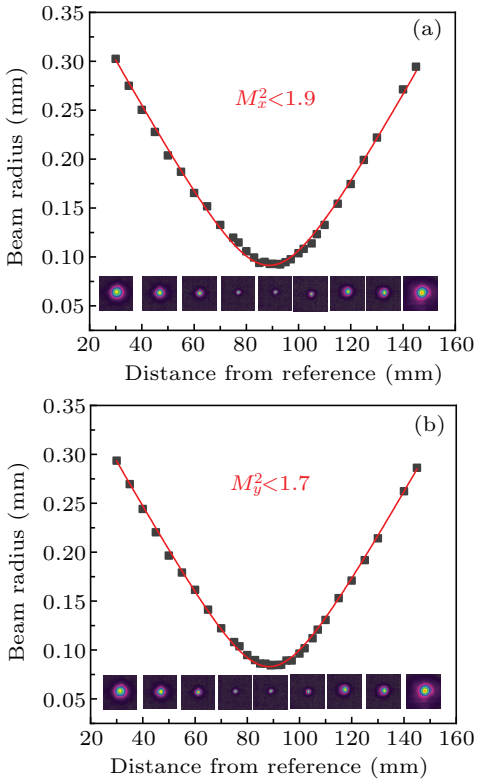


Fig. 5. Beam profile measurement of signal in horizontal (a) and vertical (b) planes.

The beam quality of the commercial pump is with $M^2 < 1.5$. To investigate the beam quality of the signal, we measured the variation of beam profile with a lens of focal length 100 mm recorded by a commercially available beam profiling camera (SP907, Ophir). Limited by the attenuation devices, the signal power was set to ∼ 800 mW. Insets in Fig. 5 are the signal beam profiles at different positions, intuitively reflecting the beam distribution and variation with diverse locations. Intensive measurements were performed near the focus, and the results are presented in Fig. 5. With Gaussian fitting, the beam propagation factor M^2 was obtained to be ∼ 1.9 and 1.7 in horizontal and vertical axes, respectively. The identical beam radii in the horizontal and vertical axes indicate an excellent spot roundness. Because of the severe thermal lensing,

the standing wave cavity is more challenging to obtain a good beam quality than the ring cavity. The $M^2 < 1.9$ ($M_x^2 < 1.9$, $M_y^2 < 1.7$) of the signal was obtained by precise adjustment of the cavity mirrors, which was close to the beam quality of the pump.

4. Conclusions

In summary, we have demonstrated a Watt-level PPKTP-based SRO-OPO with a pulse duration of ~ 1.0 ns. The maximum output power of signal is 1.51 W with maximum extraction efficiency up to 59%. The build-up time of OPO is estimated to be 1.6 ns with twin-peak pulse profile of pump. A good beam propagation factor M^2 in horizontal and vertical planes is obtained with excellent Gaussian fitting. Furthermore, the expected improvement of output power, beam quality, and extraction efficiency could be obtained by selecting a better pump source. This OPO laser will be applied to our DUV laser at 193 nm by sum-frequency generation with 266 nm in the following experimental research.

Acknowledgements

The work was supported by the Chinese Academy of Sciences Pioneer Hundred Talents Program (Grant No. E1Z1D101) and the Research Project of Aerospace Information Research Institute, Chinese Academy of Sciences (Grant No. E2Z2D101).

References

[1] Freudiger C W, Min W, Saar B G, Lu S, Holtom G R, He C, Tsai J C, Kang J X and Xie X S 2008 *Science* **322** 1857
[2] Zhu S, Chen X, Liu X, Zhang G and Tian P 2020 *Prog. Quantum Electron.* **73** 100274
[3] Arslanov D D, Spunei M, Mandon J, Cristescu S M, Persijn S T and Harren F J 2013 *Laser Photon. Rev.* **7** 188
[4] Ni R, Du L, Wu Y, Hu X P, Zou J, Sheng Y, Arie A, Zhang Y and Zhu S N 2016 *Appl. Phys. Lett.* **108** 031104
[5] Kornienko V V, Kitaeva G K, Sedlmeir F, Leuchs G and Schwefel H G L 2018 *APL Photon.* **3** 051704
[6] Yan C, Wang Y, Xu D, Xu W, Liu P, Yan D, Duan P, Zhong K, Shi W and Yao J 2016 *Appl. Phys. Lett.* **108** 011107
[7] Bae I H, Moon H S, Kim S K, Park S N and Lee D H 2012 *Appl. Phys. B* **106** 797
[8] Zhang J, Fai Mak K, Nagl N, Seidel M, Bauer D, Sutter D, Pervak V, Kraus F and Pronin O 2018 *Light Sci. Appl.* **7** 17180
[9] Li Y J, Liu Q, Feng J X and Zhang K S 2013 *Chin. Phys. B* **22** 064214
[10] Kumar S C and Ebrahim-Zadeh M 2020 *Opt. Lett.* **45** 6486
[11] X C Wang, Wang Y H, Zheng H, Liu H Z, Yu Y J and Wang Z J 2021 *Current Opt. Photon.* **5** 59
[12] Nandy B, Kumar S C and Ebrahim-Zadeh M 2020 *Opt. Lett.* **45** 6126
[13] Bierlein J D and Vanherzeele H 1989 *J. Opt. Soc. Am. B* **6** 622
[14] Kores C C, Canalias C and F Laurell 2021 *APL Photon.* **6** 091102
[15] Weise D, Strößner U, Peters A, Mlynek J, Schiller S, Arie A, Skliar A and Rosenman G 2000 *Opt. Commun.* **184** 329
[16] Garashi A, Arie A, Skliar A and Rosenman G 1998 *Opt. Lett.* **23** 1739
[17] Strößner U, Meyn J P, Wallenstein R, Urenski P, Arie A, Rosenman G, Mlynek J, Schiller S and Peters A 2002 *J. Opt. Soc. Am. B* **19** 1419
[18] Kumar S C, Parsa S and Ebrahim-Zadeh M 2016 *Opt. Lett.* **41** 52
[19] Devi K, Padhye A and Ebrahim-Zadeh M 2019 *Opt. Express* **27** 24093